ISSN 1330-3651 (Print), ISSN 1848-6339 (Online)
Received: 15 July 2025; Accepted: 14 September 2025

https://doi.org/10.17559/TV-20250715002834
Original scientific paper

Investigation of Dimensional Deviations in SLA 3D-Printed Cylindrical Features

Josip KAČMARČIK*, Kenan VARDA, Ernad BEŠLAGIĆ, Pejo KONJATIĆ

Abstract: Dimensional accuracy is a critical challenge across many additive manufacturing (AM) technologies, directly impacting the assembly of 3D-printed parts. This study investigates these deviations for stereolithography (SLA) on a desktop printer. To analyse the influence of part geometry and the key process parameter of layer thickness, 54 specimens featuring cylindrical protrusions and holes (5, 10, and 20 mm nominal diameters) were produced with three distinct thickness values (25, 50, and 100 µm). A Coordinate Measuring Machine (CMM) was used to measure dimensional and geometric characteristics, and Analysis of Variance (ANOVA) was performed for statistical analysis. The results revealed a systematic deviation trend: protrusions were consistently oversized (up to +195 µm), while holes were consistently undersized (down to –250 µm). Both diameter and layer thickness were found to be statistically significant parameters influencing these deviations. Based on these findings, a compensation strategy was developed to correct CAD models by accounting for mean deviation and process variability. The strategy was successfully verified through a practical example, demonstrating its effectiveness in achieving a controlled clearance fit (26 µm). This approach provides a practical methodology for improving the functional accuracy of SLA parts, crucial for a wide range of engineering applications where precise component assembly is required, including the production of functional prototypes and custom spare parts.

Keywords: 3D printing; ANOVA; clearance fit; compensation strategy; dimensional accuracy; stereolithography (SLA)

1 INTRODUCTION

Additive manufacturing (AM), for which 3D printing is a frequently used synonym, is an important technology for Industry 4.0 and the transition to digital manufacturing [1-7]. As a digital technology, AM relies on digital models to fabricate physical objects. Its applications include, among others, rapid prototyping, the production of customized parts, and the creation of complex geometries [8].

Stereolithography (SLA) is considered the pioneering AM technology, with its origins dating back to the 1980s. It is recognized for its ability to produce parts with high resolution and detail [9, 10], making it a preferred choice in industries where precision is crucial. This process utilises a photopolymer resin, typically a thermosetting polymer, which selectively cures and solidifies when exposed to a light source, often a UV laser. In this manner, the 3D part is built by solidifying the material layer by layer. According to ISO/ASTM 52900:2021, SLA is classified under vat polymerization processes, so named because the photopolymer, in its liquid state, is contained in a vat during the build process.

Dimensional accuracy remains a significant challenge across various additive manufacturing technologies, including SLA [11, 12], mostly due to a combination of thermal and chemical shrinkage inherent in these fabrication methods. The dimensional fidelity of SLA-printed parts is influenced by several factors, such as processing parameters, layer thickness, build orientation, and the properties of the photopolymer materials used [13]. For instance, while thinner layers are often associated with improved surface finish and potential precision, their direct correlation with optimal dimensional accuracy is not always guaranteed and requires careful consideration [14]. Previous studies have quantified typical dimensional deviations for SLA parts being in the range of 50 to 150 µm, depending on geometry and process conditions [9, 12]. A commonly reported systematic issue is the undersizing of internal features like holes, often attributed to phenomena such as localised over-curing and material shrinkage [11, 15]. Furthermore, the choice and characteristics of the resin significantly affect the curing process and, consequently, the dimensional integrity and final properties of the printed parts [13, 15].

This study investigated the dimensional accuracy achievable with the Formlabs Form 3 desktop SLA printer. Specifically, it focused on the precision of cylindrical features and the printer's capability to produce parts that met different fit tolerances. Cylindrical features such as shafts and holes are fundamental to a vast range of mechanical assemblies, making the control of their dimensional accuracy a critical factor for the functional application of 3D-printed parts.

To systematically investigate geometric deviations, a total of 54 specimens were fabricated for this study. The specimens featured cylindrical protrusions (i.e., shafts) and holes of three nominal diameters (5, 10, and 20 mm). Furthermore, to examine the influence of a key printing parameter, all specimens were produced with three distinct layer thicknesses (25, 50, and 100 µm). The resulting dimensional accuracy was then evaluated through precise measurements conducted on a Coordinate Measuring Machine (CMM). Part orientation, while recognized from literature as another influential parameter affecting overall part quality [13], was not an experimental variable in this research; instead, recommendations from the manufacturer for the most favourable orientation were adopted [16].

Based on the measurement results, this paper proposes a practical compensation strategy to correct for the observed deviations and reliably achieve controlled clearance fits. This approach therefore offers a valuable method for producing functional parts with direct industrial application, particularly in the assembly of precise mechanical components. Finally, the effectiveness of this strategy is confirmed through a preliminary experimental validation, demonstrating a practical methodology for achieving controlled clearance fits.

2 EXPERIMENTAL SET-UP

2.1 Design of Specimens' CAD Models

Test specimens were designed featuring either a cylindrical protrusion (shaft) or a cylindrical hole on a

square base. The nominal diameters for these cylindrical features were selected as 5 mm, 10 mm, and 20 mm. These dimensions were chosen based on the printer's build volume and to cover a common range of feature sizes expected for parts fabricated using the investigated printer. All CAD models were created using SolidWorks software (Dassault Systèmes).To achieve a baseline loose fit, the diameter of the protrusions was reduced by 50 μm, 75 μm, and 100 μm for the 5, 10, and 20 mm nominal diameters, respectively. The selected reduction values were based on a pragmatic estimation of the printer's dimensional performance. This resulted in final CAD dimensions of 4,95; 9,925; and 19,9 mm, as shown in the technical drawing in Fig. 1. Correspondingly, the cylindrical hole specimens were designed with nominal diameters of 5, 10, and 20 mm, as presented in the technical drawing in Fig. 2. The side length of the specimens' square bases was set to be 10 mm larger than the nominal diameter of the respective cylindrical feature. For all specimens, the height of the cylindrical protrusions and the depth of the cylindrical holes were designed to be 15 mm. This 15 mm dimension was chosen to ensure an adequate geometric feature for testing purposes, while also maintaining a reasonable specimen size for 3D printing, particularly in terms of production time. Additionally, to facilitate secure clamping of the specimens during measurements on a Coordinate Measuring Machine (CMM), two small extensions were added at the bottom of each model's base. Each CAD model also included an engraved Specimen ID (the specifics of which will be detailed later in the text); this ID served to denote the specimen's particular geometry and the layer thickness to be used for 3D printing.

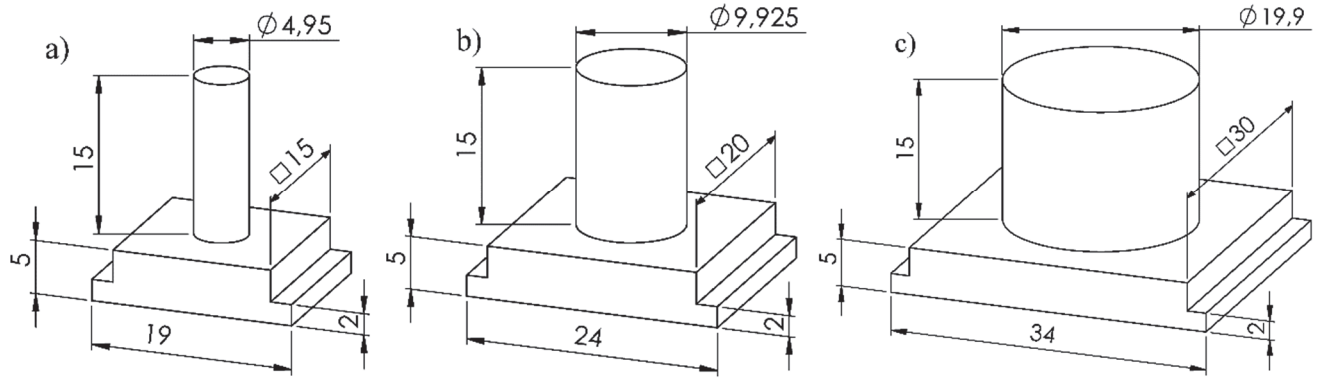

Figure 1 Design of test specimens with a cylindrical protrusion in nominal dimensions: a) 5 mm; b) 10 mm and c) 20 mm

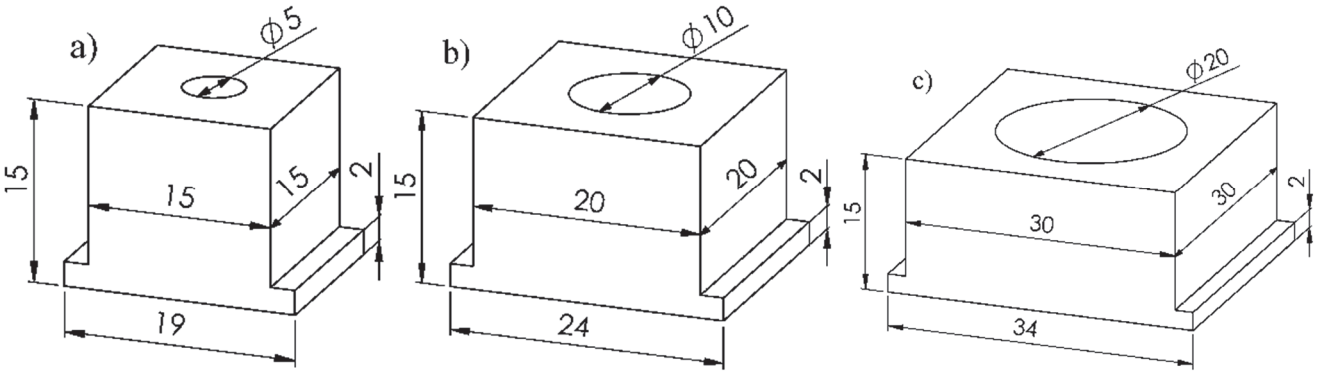

Figure 2 Design of test specimens with a cylindrical hole in nominal dimensions: a) 5 mm; b) 10 mm and c) 20 mm

2.2 3D Printing and Experimental Plan

For the fabrication and post-processing of specimens, a Formlabs Form 3 3D printer [17], a Form Wash unit [18], and a Form Cure unit [19] were utilised. This equipment setup is shown in Fig. 3. The specimens were produced using Grey Resin V4 [20]. Each nominal dimension of the specimens was printed using three different layer thicknesses, with three replicates fabricated for each combination of parameters. Consequently, a total of 54 specimens were produced (2 feature types × 3 nominal dimensions × 3 layer thicknesses × 3 replicates). All specimens, along with their specific parameters and the designations used in this study, are detailed in Tab. 1.

Print setup was performed using Formlabs' PreForm software [21]. The specimens were printed in batches, a methodological choice that represents a known limitation when compared to the standard metrological practice of fabricating each specimen individually. However, this method was chosen because it facilitates efficient production and saves processing time, thereby reflecting a typical 3D printing scenario and enhancing the practical relevance of the study's findings. To obtain the three required replicates for each unique specimen design, a combination of two print layouts was used for each layer thickness. The specific layouts for the 50 μm layer thickness are presented in Figs. 4 and 5 as an example, and similar layouts were used for the other thicknesses. For all models, the manufacturer's recommendation to orient large, flat surfaces at an incline of 10-20° [16] was followed; specifically, the base surfaces of the models were tilted at a 15° angle relative to the build plate.

Table 1 Experimental plan

Specimen Type	Diameter / mm	Layer Thickness / µm	Specimen IDs	Number of Replicates
Cylindrical protrusions	4,95	25	C5-1-a, C5-1-b, C5-1-c	3
		50	C5-2-a, C5-2-b, C5-2-c	
		100	C5-3-a, C5-3-b, C5-3-c	
	9,925	25	C10-1-a, C10-1-b, C10-1-c	
		50	C10-2-a, C10-2-b, C10-2-c	
		100	C10-3-a, C10-3-b, C10-3-c	
	19,9	25	C20-1-a, C20-1-b, C20-1-c	
		50	C20-2-a, C20-2-b, C20-2-c	
		100	C20-3-a, C20-3-b, C20-3-c	
Cylindrical holes	5	25	O5-1-a, O5-1-b, O5-1-c	
		50	O5-2-a, O5-2-b, O5-2-c	
		100	O5-3-a, O5-3-b, O5-3-c	
	10	25	O10-1-a, O10-1-b, O10-1-c	
		50	O10-2-a, O10-2-b, O10-2-c	
		100	O10-3-a, O10-3-b, O10-3-c	
	20	25	O20-1-a, O20-1-b, O20-1-c	
		50	O20-2-a, O20-2-b, O20-2-c	
		100	O20-3-a, O20-3-b, O20-3-c	

Figure 3 Formlabs form 3 setup: a) Form 3 printer; b) Form wash and c) Form cure

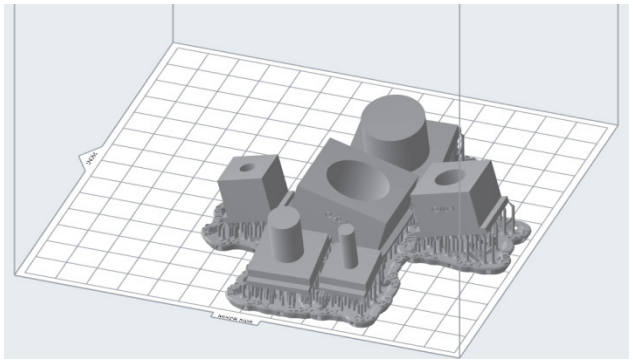

Figure 4 3D printing layout with one specimens design replica (50 µm layer)

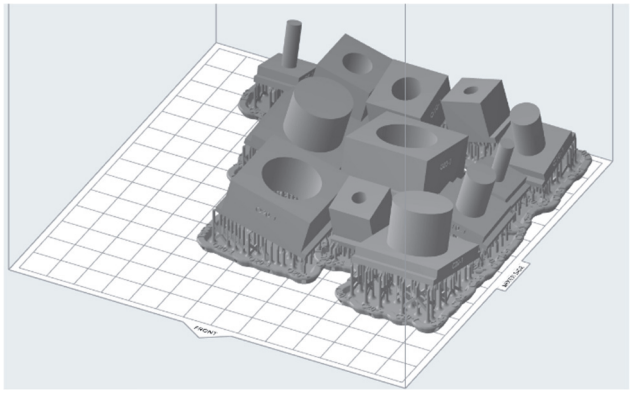

Figure 5 3D printing layout with two specimens design replicas (50 µm layer)

Post-processing of the printed specimens involved cleaning in a Form Wash unit using isopropyl alcohol (IPA) as the solvent, followed by UV post-curing in a Form Cure unit. For the post-curing process the manufacturer's recommendations for full cure were followed: 60 minutes at 60 °C [22]. The fabricated specimens after completion of all post-processing steps are shown in Fig. 6.

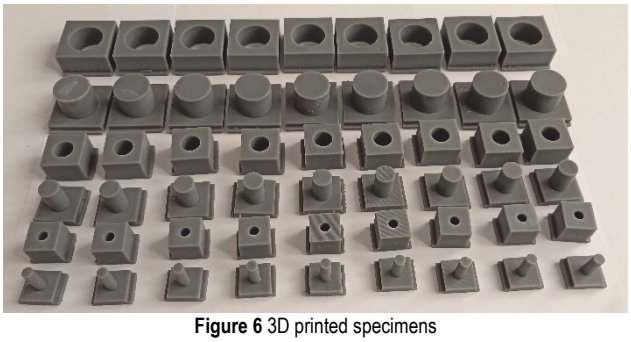

Figure 6 3D printed specimens

A physical inspection of the fabricated specimens revealed generally good surface quality across most areas. Exceptions were observed only on surfaces where support structures were attached. However, during the print setup, specimens were oriented in such a way (Figs. 4 and 5) to avoid placing supports on the cylindrical features central to this research. Consequently, these support-affected surfaces, where small remnants of supports remained, did not require additional processing or grinding, because of their negligible impact on the dimensions of the features under investigation. Significantly, it was noted that the pragmatically defined diameter reductions applied to the cylindrical protrusions were insufficient to enable assembly with their corresponding hole specimens and achieve a loose fit. A more precise determination of the actual overlap will be established through subsequent CMM dimensional measurements.

2.3 Measurement Methodology

Dimensional measurements were performed using a Zeiss Contura G2 Coordinate Measuring Machine (CMM) equipped with a ZEISS VAST XT probe (see Fig. 7). For specimens with a 5 mm nominal diameter, a stylus with a 1,5 mm ruby tip was employed (Fig. 8a). For the larger nominal diameters of 10 mm and 20 mm, a stylus with a 2 mm ruby tip was used (Fig. 8b).

Figure 7 Zeiss Contura G2 CMM with ZEISS VAST XT probe

All measurement processes and strategies definition, as well as measured data evaluation were managed using ZEISS CALYPSO software. Workpiece alignment within the software was initially performed manually. This involved manual measurement of single points on the cylindrical features and reference planar surfaces. These manually measured features served as the basis for establishing the part's coordinate system. Manual alignment and measurement were performed for only one representative specimen of each type and nominal dimension. Subsequent measurements of the remaining replicates were entirely automated. For this purpose, a custom-designed fixture was utilised, consisting of a wooden base plate and 3D-printed clamps that securely held the specimens and could be tightened with screws (Fig. 8). This setup facilitated repeatable and automated measurement of multiple specimens.

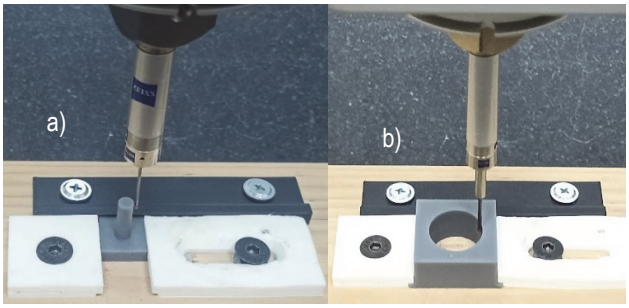

Figure 8 Measurement of a feature on a fixed sample: a) a 5 mm diameter cylinder using a stylus with a 0.8 mm silicon nitride tip; b) a 20 mm diameter hole using a stylus with a 2 mm ruby tip

Cylindrical features (both protrusions and holes) were measured using a scanning strategy commonly referred to as a 'bird cage' strategy, as recommended in ISO 12180. This specific strategy involved collecting data along two circular paths with a vertical separation of 5 mm (where the upper circular path was positioned a few millimetres below the top edge of the cylindrical feature) and four vertical lines (Fig. 9). To avoid stylus body collisions (often referred to as 'trunking'), data collection was intentionally limited to the upper regions of the features, even though the cylindrical features were 15 mm high. Planar surfaces were measured using a single points measurement strategy, collecting 8 points on each surface via touch-trigger probing (Fig. 10).

For cylindrical protrusions (shafts), the diameter was determined using the Minimum Circumscribed Circle (MCC) algorithm. Conversely, for cylindrical holes, the Maximum Inscribed Circle (MIC) algorithm was applied for diameter calculation. The measured characteristics, as defined within the CALYPSO software, included the diameter of the cylindrical features, and also their cylindricity, and their perpendicularity relative to the reference planar surfaces. These measured results will be presented and analysed in the subsequent chapter.

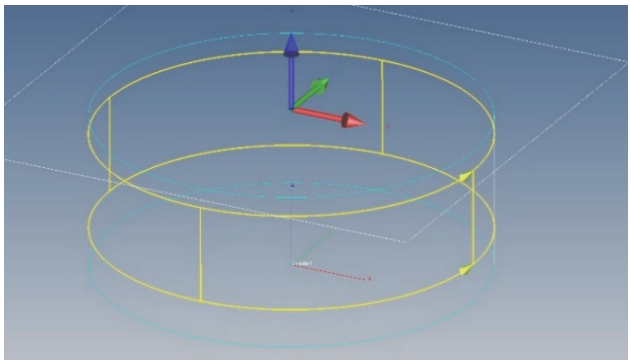

Figure 9 'Bird cage' measurement strategy in ZEISS CALYPSO software (example for a 20 mm hole specimen)

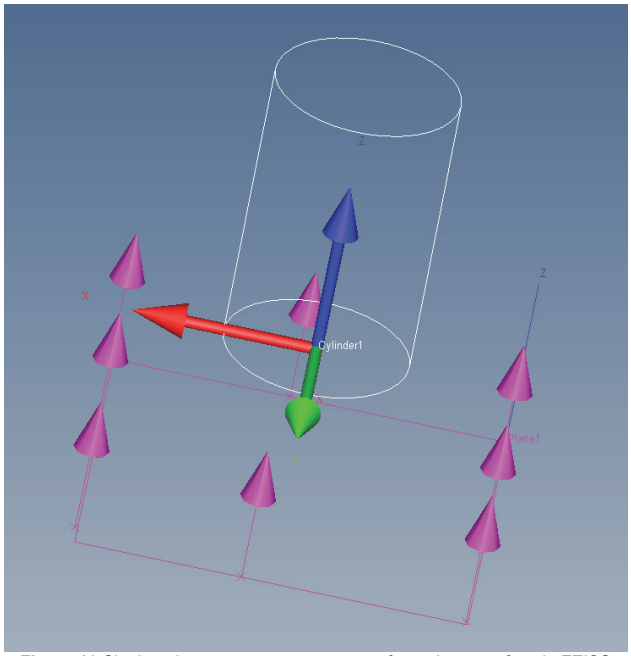

Figure 10 Single points measurement strategy for a planar surface in ZEISS CALYPSO software (example for a 5 mm protrusion specimen)

3 RESULTS

3.1 CMM Results

Based on CMM measurement results for the three repetitions of each experimental combination, mean values and standard deviations were calculated for the diameter, cylindricity, and perpendicularity of the cylindrical features. Furthermore, the deviation from the nominal CAD dimensions was determined. These key results are presented in Tab. 2 for cylindrical protrusions and Tab. 3 for cylindrical holes, and graphically visualised in Figs. 11 to 15. The error bars in the figures represent the standard deviation of the three replicates for each combination of nominal diameter and layer thickness.

The measurement data shows a consistent positive dimensional deviation (oversizing) for all cylindrical protrusions, with mean values ranging from approximately 95 µm to 195 µm. Conversely, all cylindrical holes

exhibited a negative deviation (undersizing), with mean values ranging from approximately –150 µm to –265 µm. This confirms a systematic deviation trend where material accumulation occurs on external features, while material shrinkage dominates in internal features.

Table 2 Measurement results for specimens with cylindrical protrusions: mean values ($\bar{x}$) and standard deviations (s)

Specimen IDs	Diameter / mm		Diameter deviation / µm		Cylindricity / µm		Perpendicularity / µm	
	$\bar{x}$	s	$\bar{x}$	s	$\bar{x}$	s	$\bar{x}$	s
C5-1-a, C5-1-b, C5-1-c	5,086	0,0081	136,27	8,12	36,53	8,89	67,31	22,22
C5-2-a, C5-2-b, C5-2-c	5,073	0,0108	122,87	10,75	42,47	10,13	46,25	14,79
C5-3-a, C5-3-b, C5-3-c	5,063	0,0395	112,68	39,52	57,99	9,53	71,3	36,92
C10-1-a, C10-1-b, C10-1-c	10,063	0,0070	137,95	7,03	60,17	13,7	121,35	80,7
C10-2-a, C10-2-b, C10-2-c	10,053	0,0152	128,31	15,2	75,77	23,09	155,56	77,14
C10-3-a, C10-3-b, C10-3-c	10,020	0,0177	94,98	17,71	63,05	19,03	89,07	52,5
C20-1-a, C20-1-b, C20-1-c	20,093	0,0079	193,24	7,86	104,13	43,56	66,98	48,02
C20-2-a, C20-2-b, C20-2-c	20,036	0,0145	136,31	14,52	92,22	7,79	57,02	7,41
C20-3-a, C20-3-b, C20-3-c	20,019	0,0271	119,02	27,09	115,98	25,16	71,89	52,41

Table 3 Measurement results for specimens with cylindrical holes: mean values ($\bar{x}$) and standard deviations (s)

Specimen IDs	Diameter / mm		Diameter deviation / µm		Cylindricity / µm		Perpendicularity / µm	
	$\bar{x}$	s	$\bar{x}$	s	$\bar{x}$	s	$\bar{x}$	s
O5-1-a, O5-1-b, O5-1-c	4,846	0,0168	–153,74	16,8	42,08	10,3	19,87	18,56
O5-2-a, O5-2-b, O5-2-c	4,800	0,0232	–200,49	23,23	82,11	34,76	36,48	9,63
O5-3-a, O5-3-b, O5-3-c	4,839	0,0674	–160,60	67,44	82,66	35,59	27,74	9,04
O10-1-a, O10-1-b, O10-1-c	9,845	0,0231	–155,13	23,12	64,55	10,36	34,14	19,6
O10-2-a, O10-2-b, O10-2-c	9,779	0,0030	–221,41	2,95	92,56	13,61	22,49	8,28
O10-3-a, O10-3-b, O10-3-c	9,838	0,0588	–162,13	58,82	92,12	18,28	19,57	2,55
O20-1-a, O20-1-b, O20-1-c	19,810	0,0072	–190,03	7,16	82,85	18,2	46,79	8,38
O20-2-a, O20-2-b, O20-2-c	19,734	0,0498	–265,78	49,84	115,53	38,51	47,21	26,98
O20-3-a, O20-3-b, O20-3-c	19,787	0,0642	–213,19	64,23	122,36	27,43	66,65	28,53

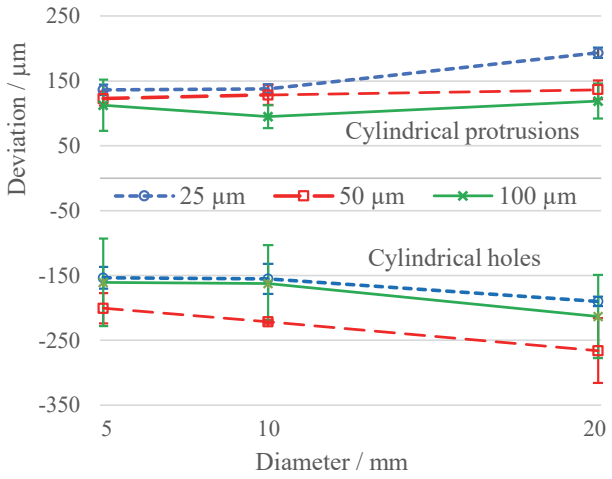

Figure 11 Dimensional deviations of SLA 3D-printed cylindrical protrusions and holes vs. nominal diameter for different layer thicknesses

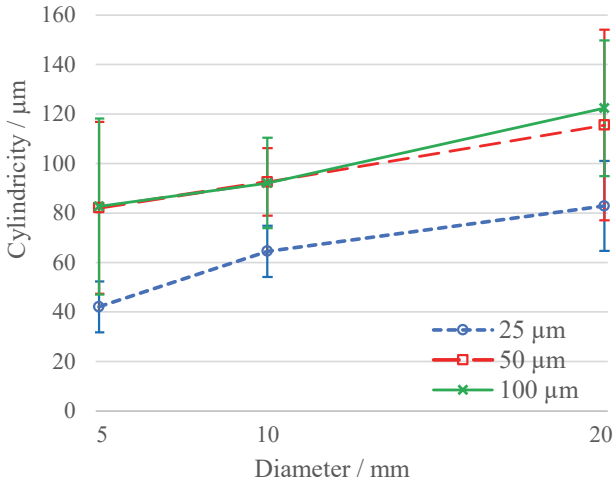

Figure 13 Cylindricity of SLA 3D-printed cylindrical holes vs. nominal diameter for different layer thicknesses

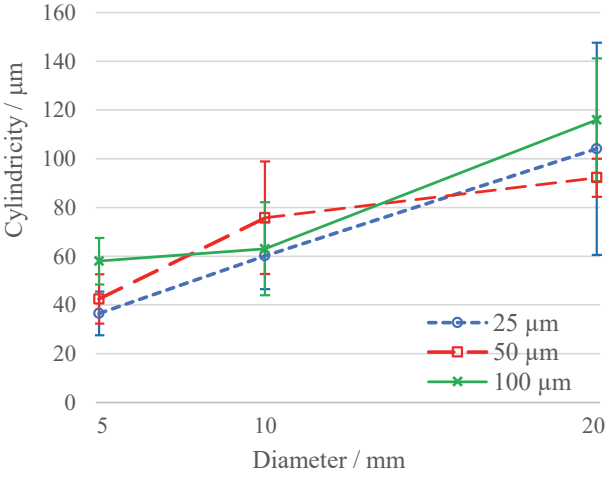

Figure 12 Cylindricity of SLA 3D-printed cylindrical protrusions vs. nominal diameter for different layer thicknesses

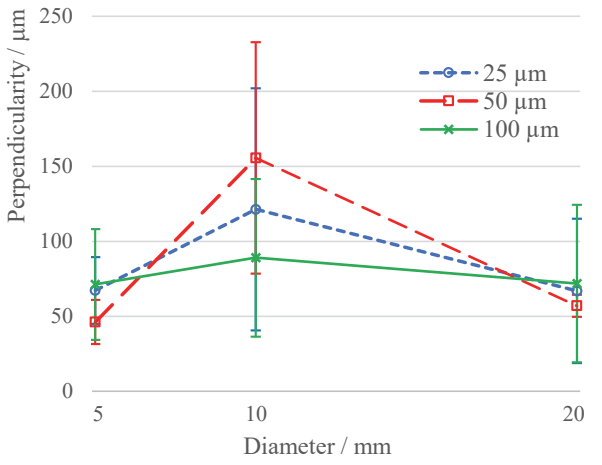

Figure 14 Perpendicularity of SLA 3D-printed cylindrical protrusions vs. nominal diameter for different layer thicknesses

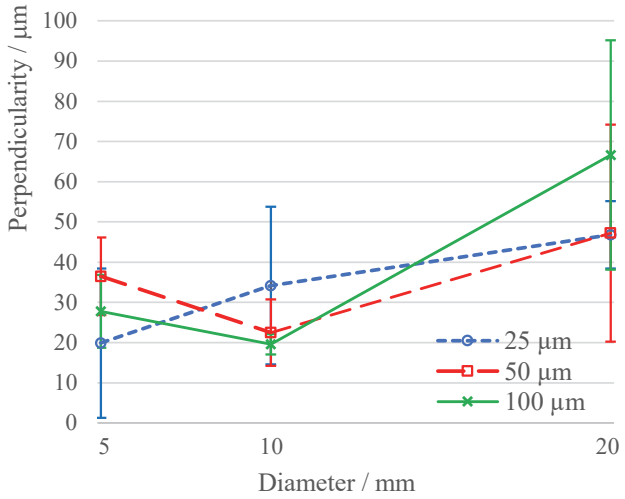

Figure 15 Perpendicularity of SLA 3D-printed cylindrical holes vs. nominal diameter for different layer thicknesses

Regarding form tolerances, the measured cylindricity values ranged from 36 µm to 116 µm for protrusions and from 42 µm to 122 µm for holes. Perpendicularity values ranged from 46 µm to 156 µm for protrusions and from 20 µm to 67 µm for holes.

3.2 ANOVA Analysis

A two-way Analysis of Variance (ANOVA) with replication was conducted using Microsoft Excel's Data Analysis ToolPak to statistically evaluate the effects of nominal diameter and layer thickness on the measured dimensional characteristics (deviation, cylindricity, and perpendicularity). The main results of the ANOVA, including *F*-values, *p*-values, and statistical significance, are summarised in Tab. 4. Statistical significance was assessed at a significance level (alpha, α) of 0.05. A p-value less than 0.05 indicates a statistically significant effect, leading to the rejection of the null hypothesis, and is denoted by 'YES' in the 'Significance ($p < 0.05$)' column of the table. Conversely, a *p*-value greater than or equal to 0.05 indicates no statistically significant effect, and is denoted by 'NO'. As presented in Tab. 4, the ANOVA results reveal which factors were statistically significant. For dimensional deviation in both protrusions and holes, both Layer thickness and Diameter had a significant effect ($p < 0.05$). Conversely, for the perpendicularity of protrusions, neither of the selected factors showed a statistically significant influence.

Table 4 ANOVA Results

Feature	Dependent Variable	Source of Variation	Sum of squares (SS)	df	Mean square (MS)	*F*-value	*P*-value	F crit	Significance ($p < 0.05$)
Cylindrical protrusions	Dimensional deviation	Layer thickness	9,970E^{-03}	2	4,985E^{-03}	13,417	0,0003	3,555	YES
		Diameter	4,543E^{-03}	2	2,272E^{-03}	6,113	0,0094	3,555	YES
		Interaction	2,968E^{-03}	4	7,419E^{-04}	1,997	0,1382	2,928	NO
	Cylindricity	Layer thickness	7,028E^{-04}	2	3,514E^{-04}	0,801	0,4640	3,555	NO
		Diameter	1,581E^{-02}	2	7,905E^{-03}	18,029	0,0001	3,555	YES
		Interaction	1,295E^{-03}	4	3,237E^{-04}	0,738	0,5781	2,928	NO
	Perpendi–cularity	Layer thickness	4,206E^{-04}	2	2,103E^{-04}	0,084	0,9193	3,555	NO
		Diameter	2,062E^{-02}	2	1,031E^{-02}	4,142	0,0331	3,555	YES
		Interaction	7,644E^{-03}	4	1,911E^{-03}	0,768	0,5601	2,928	NO
Cylindrical holes	Dimensional deviation	Layer thickness	2,001E^{-02}	2	1,001E^{-02}	5,617	0,0127	3,555	YES
		Diameter	1,377E^{-02}	2	6,887E^{-03}	3,866	0,0401	3,555	YES
		Interaction	8,071E^{-04}	4	2,018E^{-04}	0,113	0,9762	2,928	NO
	Cylindricity	Layer thickness	7,261E^{-03}	2	3,630E^{-03}	5,658	0,0124	3,555	YES
		Diameter	6,628E^{-03}	2	3,314E^{-03}	5,165	0,0169	3,555	YES
		Interaction	2,090E^{-04}	4	5,224E^{-05}	0,081	0,9871	2,928	NO
	Perpendi–cularity	Layer thickness	8,765E^{-05}	2	4,383E^{-05}	0,152	0,8599	3,555	NO
		Diameter	4,352E^{-03}	2	2,176E^{-03}	7,561	0,0041	3,555	YES
		Interaction	1,455E^{-03}	4	3,638E^{-04}	1,264	0,3203	2,928	NO

4 DISCUSSION

4.1 Dimensional and Form Deviations

The results confirmed a systematic dimensional deviation between the 3D-printed parts and their nominal CAD models. The findings of this study show that cylindrical protrusions were consistently oversized, while cylindrical holes were undersized. This observation is consistent with the findings from previous research [9, 12, 13]. As detailed in the results section, the average dimensional deviations were consistently positive for protrusions and negative for holes, with magnitudes reaching up to approximately 195 µm and –265 µm, respectively (Tabs. 2 and 3). These deviation magnitudes are also in line with previous studies. From this clear distinction between the directional deviation of external and internal features, it can be concluded that this is an inherent characteristic of the SLA process. The observed deviations also confirm the initial physical assessment that the pre-defined allowances for achieving a loose fit were insufficient.

The reasons for these inaccuracies are inherent to the nature of the SLA process. The main phenomena influencing the final accuracy are material shrinkage and the curing process [9, 12-14]. Shrinkage is the volume reduction of the resin as it solidifies, while curing is the solidification of the resin under UV light, a process that also introduces dimensional changes. Together, these phenomena introduce deformations and residual stresses into the material. This happens both during the layer-by-layer 3D printing and during the subsequent UV post-curing stage, ultimately leading to the dimensional changes and geometric inaccuracies observed in the final printed part.

Regarding the form tolerances, the measured values for cylindricity and perpendicularity, as detailed in Tabs. 2 and 3, also showed significant variation and deviation from the nominal geometry.

The influence of printing parameters on the final accuracy was analysed using ANOVA (Tab. 4). For dimensional deviation, both layer thickness and nominal diameter showed a statistically significant effect for both protrusions and holes. However, although it might be expected that smaller layer thicknesses and smaller nominal diameters would lead to higher dimensional accuracy, this was not consistently observed in the results. This lack of a clear trend may be due to several factors. The simple geometry of the specimens could reduce the overall effect of layer thickness. Also, the influence of other parameters, combined with the fact that statistical deviations can sometimes be larger than the effect of the printing parameters, can make the significance of their influence not clearly visible.This is supported by the error bars in the figures (Figs. 11 to 15), which, while generally indicating acceptable process repeatability, are larger in some cases, particularly for perpendicularity, suggesting a wider spread of results can occur.

For form tolerances, the ANOVA results show a more variable influence of the printing parameters. For cylindrical protrusions, only the diameter had a statistically significant effect on both cylindricity and perpendicularity, while layer thickness did not show a significant influence. For cylindrical holes, both diameter and layer thickness had a significant effect on cylindricity, but only diameter had a significant effect on perpendicularity. Similar to the dimensional deviations, a clear trend that smaller dimensions and thinner layers consistently produce better form accuracy was not established, likely for similar reasons. Generally, it can be observed from Figs. 11 to 15 that dimensional and form accuracy tends to decrease with larger layer thicknesses and larger nominal diameters, but this trend is not clearly visible for all measured characteristics. It is also important to note that for all analysed features, no statistically significant interaction between layer thickness and diameter was found, indicating that the effect of one parameter does not significantly depend on the level of the other.

To summarise, the observed dimensional and form deviations are acceptable and fall within the expected range for desktop SLA 3D printing technology. However, the results clearly show that if users want to produce parts for assemblies that require a specific fit or have specific requirements for dimensional and form tolerances, they must apply corrections to the nominal CAD models before printing.

4.2 Dimensional Compensations for Loose Fits

The results from this study confirm that corrections to the nominal CAD dimensions are necessary in order to achieve loose fits for cylindrical features in assemblies, which is a common requirement for 3D-printed parts. These corrections compensate for the dimensional deviations inherent in the SLA 3D printing process. Since the ANOVA results showed that these deviations were dependent on both layer thickness and nominal diameter, different correction values should be defined for each unique combination of these parameters.

This study adopts a compensation strategy combining two components for each parameter set. These components are the mean diameter deviation ($\overline{\Delta_p}$, Tab. 2) and a clearance allowance (δ_p). The mean dimeter deviations are positive values for protrusions and negative values for holes. The factor δ_p accounts for both the desired minimum clearance and the statistical stability of the process, i.e., the standard deviation of the diameter deviations (Tab. 2). The value of the allowance is determined using a straightforward "worst-case scenario" approach. It is calculated as the sum of the standard deviations for both the protrusion (s_C) and the hole (s_O), to which a minimum required clearance of 10 µm is added. To create a set of simple and practical design rules, a minimum recommended allowance of 50 µm was adopted. For cases requiring a larger allowance, subsequent values were selected from a series with an increment of 25 µm (i.e., 75 µm, 100 µm, 125 µm). For assembly, the factor δ_p is divided equally between the protrusion and the hole. The required values for the clearance allowance for each parameter combination are calculated and presented in Tab. 5.

Table 5 Calculation of the recommended clearance allowance

Nominal diameter / mm	Layer thickness / µm	Standard deviation of diameter deviation / µm		Calculated clearance allowance / µm ($s_C + s_O + 10$ µm)	Recommended clearance allowance δ_p / µm
		Protrusion, s_C	Hole, s_O		
5	25	8,12	16,8	34,92	50
	50	10,75	23,23	43,98	50
	100	39,52	67,44	116,96	125
10	25	7,03	23,12	40,15	50
	50	15,2	2,95	28,15	50
	100	17,71	58,82	86,53	100
20	25	7,86	7,16	25,02	50
	50	14,52	49,84	74,36	75
	100	27,09	64,23	101,32	125

Finally, the formulas for calculating the corrected diameters to be used in CAD models for cylindrical protrusions are:

$$d_{\mathrm{CAD}} = d_{\mathrm{nom}} - \overline{\Delta_p} - \delta_p / 2 \tag{1}$$

and for cylindrical holes:

$$D_{\mathrm{CAD}} = D_{\mathrm{nom}} - \overline{\Delta_p} - \delta_p / 2 \tag{2}$$

where d_{nom}, D_{nom} are the nominal diameters for the protrusion and hole, $\overline{\Delta_p}$ is the mean measured deviation (Tabs. 2 and 3) and δ_p is recommended clearance allowance (Tab. 5).

4.3 Experimental Validation

To perform a preliminary verification and provide a practical example of the proposed compensation method, one experimental validation pair was produced. This pair consisted of a cylindrical protrusion and a corresponding hole with the same nominal geometry as the initial test specimens, as shown in Figs. 1 and 2. The mid-range printing and geometry parameters were chosen for this test: a 10 mm nominal diameter and a 50 µm layer thickness.

By applying Eq. (1) and using the data from Tabs. 2, 3 and 5 for the 10 mm diameter and 50 µm layer thickness, the corrected diameter for the protrusion is:

$$10 - 128{,}31 \cdot 10^{-3} - 25 \cdot 10^{-3} = 9{,}847 \text{ mm},$$

and for the cylindrical hole, Eq. (2):

$$10 - \left(-221{,}41 \cdot 10^{-3}\right) + 25 \cdot 10^{-3} = 10{,}246 \text{ mm}.$$

Table 6 Validation results for the compensated cylindrical protrusion-hole pair

Feature	CAD dimension / mm	Target Dimension / mm	Measured Dimension / mm	Deviation from CAD / µm	Deviation from Target / µm
Protrusion	9,847	9,975	9,987	140	12
Hole	10,246	10,025	10,012	–234	–13
Clearance	/	0,05	0,026	/	–24

The new specimens were fabricated and measured in the same manner as the initial ones, as described in Chapter 2. A preliminary visual and manual inspection confirmed that a loose fit was achieved and the parts could be assembled (Fig. 16). The measurement results - including the design dimensions used in the CAD models, the final measured dimensions, the target dimensions, the calculated deviations, and the final achieved clearance - are presented in Tab. 6.

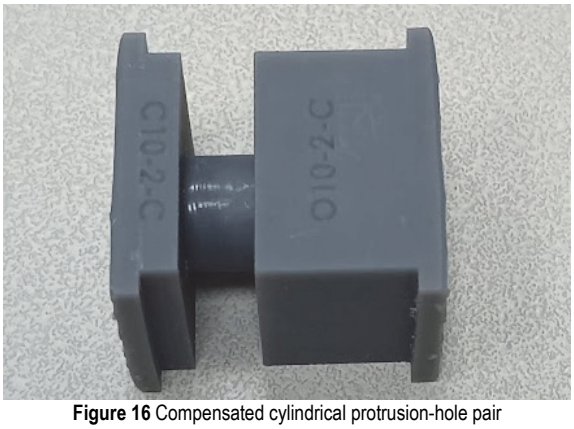

Figure 16 Compensated cylindrical protrusion-hole pair

The evaluation of the compensated specimens shows a significant improvement in dimensional accuracy compared to the initial parts. As presented in Tab. 6, the measured clearance of 26 µm, while lower than the 50 µm target, is still an acceptable value for providing a functional loose fit. The deviation from the target clearance (–24 µm) is slightly outside the predicted variability range for this specific parameter set ($s_C + s_O \approx 18$ µm). However, considering the small sample size used for the standard deviation calculations, this result falls well within the overall trends of process variability observed across all experimental conditions (Tabs. 2 and 3). This provides a positive, although preliminary, confirmation that the proposed compensation strategy is effective and can be used to produce functional assemblies with predictable loose fits.

5 CONCLUSIONS

This study investigated the dimensional accuracy of cylindrical geometries fabricated using a Formlabs Form 3 desktop SLA 3D printer. The influence of geometric dimensions (diameter) and a key SLA process parameter (layer thickness) was also examined. Based on the statistically determined deviations from the nominal dimensions, a practical strategy was proposed for correcting dimensions in the CAD model to compensate for inaccuracies and achieve a predictable loose fit.

The statistical analysis of the CMM measurement results confirmed a systematic positive deviation (oversizing) for cylindrical protrusions and a negative deviation (undersizing) for cylindrical holes. This behaviour is both explainable and expected, based on the nature of the SLA technology, which involves thermal effects and deformations due to photocuring. Furthermore, a statistically significant relationship was found between the dimensional deviation and both the geometric dimensions and the layer thickness.

Based on the statistical data from the observed deviations, a compensation strategy was proposed, involving the calculation of necessary corrections to achieve a loose fit. The correction value was defined as a sum of the mean deviation from the nominal dimensions, the process variability (represented by the standard deviation of that same deviation), and a clearance allowance to ensure a minimum gap. Additionally, the proposed allowances were rounded to practical values to facilitate engineering application. The application of this calculation was demonstrated and experimentally confirmed on a selected protrusion-hole pair.

This paper provides future users of SLA 3D printing, particularly the Formlabs Form 3 printer, with data on expected deviations and offers a clear compensation strategy for achieving loose fits. The proposed calculation is described in detail, allowing potential users to adapt it to their own needs, conditions, or even different printer behaviours, which the authors do not exclude due to the complexity of the process.

Finally, the authors wish to emphasise that these recommendations should be considered within the context of this study's limitations. The findings are based on a specific printer model, a single printer unit, one batch of material, a limited number of specimens, and a specific layout of specimens during 3D printing. Nevertheless, this research serves as a practical and valuable guide for compensating dimensional errors on cylindrical features in the SLA 3D printing process.

Acknowledgements

This research was conducted as part of the project "Investigation of the dimensional accuracy of different 3D printing technologies", which was funded by the Federal Ministry of Education and Science, Federation of BiH, Bosnia and Herzegovina.

6 REFERENCES

[1] Godina, R., Ribeiro, I., Matos, F., Ferreira, B. T., Carvalho, H., & Peças, P. (2020). Impact assessment of additive manufacturing on sustainable business models in industry 4.0 context. *Sustainability*, *12*(17), 7066. https://doi.org/10.3390/su12177066

[2] Barth, H., Krishna, A. M., Reddy, V. K., & Rosén, B. G. (2024). From traditional manufacturing to digital manufacturing: Two Swedish case studies. *Digital transformation in manufacturing*. https://doi.org/10.5772/intechopen.111862

[3] AMPOWER. (2024). *AMPOWER Report 2024, Additive Manufacturing Report*. Ampower GmbH & Co. KG. https://additive-manufacturing-report.com

[4] Srivastava, M. & Rathee, S. (2021). Additive manufacturing: Recent trends, applications and future outlooks. *Progress in Additive Manufacturing*, *7*(2), 261-287. https://doi.org/10.1007/s40964-021-00229-8

[5] Patalas-Maliszewska, J., Topczak, M., & Kłos, S. (2020). The level of the additive manufacturing technology use in Polish metal and automotive manufacturing enterprises. *Applied Sciences*, *10*(3), 735. https://doi.org/10.3390/app10030735

[6] Begic-Hajdarevic, D., Klancnik, S., Muhamedagic, K., Cekic, A., Cohodar Husic, M., Ficko, M., & Gusel, L. (2024). FDM process parameter selection by hybrid MCDM approach for flexural and compression strength maximization. *Advances in Production Engineering & Management, 19*(1), 108-116. https://doi.org/10.14743/apem2024.1.496

[7] Neuenfeldt Júnior, A., Nogueira, P., Francescatto, M., Siluk, J., De Paris, S., & Mandlhate, M. (2024). Application of a proposed additive manufacturing performance measurement system in a Brazilian industry. *International Journal of Industrial Engineering and Management, 15*(2), 109-124. https://doi.org/10.24867/IJIEM-2024-2-351

[8] Iftekar, S. F., Aabid, A., Amir, A., & Baig, M. (2023). Advancements and limitations in 3D printing materials and technologies: A critical review. *Polymers*, *15*(11), 2519. https://doi.org/10.3390/polym15112519

[9] Lu, Y., Hu, P., Wu, Z., Liu, W., Lv, Q., Nie, Z., Cen, Y., & He, Z. (2020). Comparison of accuracy and precision of various types of photo-curing printing technology. *Journal of Physics: Conference Series*, *1549*(3), 032151. https://doi.org/10.1088/1742-6596/1549/3/032151

[10] Heidt, B., Rogosic, R., Bonni, S., Passariello-Jansen, J., Dimech, D., Lowdon, J., Wady, H., Temiz, Y., & Cleij, T. J. (2020). The liberalization of microfluidics: Form 2 benchtop 3D printing as an affordable alternative to established manufacturing methods. *Physica Status SolidiA*, *217*, 1900935. https://doi.org/10.1002/pssa.201900935

[11] Mou, Y. & Koç, M. (2019). Dimensional capability of selected 3DP technologies. *Rapid Prototyping Journal*, *25*(5), 915-924. https://doi.org/10.1108/rpj-03-2019-0061

[12] Msallem, B., Vavrina, J., Beyer, M., Halbeisen, F. S., Lauer, G., Dragu, A., Luebbers, H.-T., & Thieringer, F. M. (2024). Dimensional accuracy in 3D printed medical models: A follow-up study on SLA and SLS technology. *Journal of Clinical Medicine*, *13*(19), 5848. https://doi.org/10.3390/jcm13195848

[13] Mhmood, T. A. & AL-Karkhi, N. S. (2023). A review of the stereo lithography 3D printing process and the effect of parameters on quality. *Al-Khwarizmi Engineering Journal*, *19*(2), 82-94. https://doi.org/10.22153/kej.2023.04.003

[14] Loflin, W. C., English, J. D., Borders, M. B., Harris, L. W., Moon, A. J., Holland, J. C., Roberts, J. A., & Kasper, F. K. (2019). Effect of print layer height on the assessment of 3D-printed models. *American Journal of Orthodontics and Dentofacial Orthopedics*, *156*(2), 283-289. https://doi.org/10.1016/j.ajodo.2019.02.013

[15] Saini, J. S., Dowling, L., Kennedy, J., & Trimble, D. (2020). Investigations of the mechanical properties on different print orientations in SLA 3D printed resin. *Proceedings of the Institution of Mechanical Engineers, Part C: Journal of Mechanical Engineering Science*, *234*(11), 2279-2293. https://doi.org/10.1177/0954406220904106

[16] Formlabs. (2023, April 20). Model orientation. *Formlabs Support*. https://support.formlabs.com/s/article/Model-Orientation

[17] Formlabs. (n.d.). *Formlabs professional 3D printer*. https://formlabs.com/3d-printers/professional/

[18] Formlabs. (n.d.). Form Wash (1st Gen). https://formlabs.com/store/post-processing/form-wash-1st-gen

[19] Formlabs. (n.d.). Form Cure. https://formlabs.com/store/post-processing/form-cure

[20] Formlabs. (n.d.). *Grey Resin V4*. https://formlabs.com/store/materials/grey-resin-v4/

[21] Formlabs. (n.d.). *PreForm 3D print preparation software*. https://formlabs.com/software/preform/

[22] Formlabs. (n.d.). Form Cure time and temperature settings. *Formlabs Support*. https://support.formlabs.com/s/article/Form-Cure-Time-and-Temperature-Settings

Contact information:

Josip KAČMARČIK, Associate Professor, PhD
(Corresponding author)
University of Zenica,
Faculty of Mechanical Engineering in Zenica,
Fakultetska 1, BiH-72000 Zenica, Bosnia and Herzegovina
E-mail: josip.kacmarcik@unze.ba

Kenan VARDA, Senior Assistant, MSc
University of Zenica,
Faculty of Mechanical Engineering in Zenica,
Fakultetska 1, BiH-72000 Zenica, Bosnia and Herzegovina
E-mail: kenan.varda@unze.ba

Ernad BEŠLAGIĆ, Assistant Professor, PhD
University of Zenica,
Faculty of Mechanical Engineering in Zenica,
Fakultetska 1, BiH-72000 Zenica, Bosnia and Herzegovina
E-mail: ernad.beslagic@unze.ba

Pejo KONJATIĆ, Full Professor, PhD
University of Slavonski Brod,
Mechanical Engineering Faculty in Slavonski Brod,
Trg Ivane Brlić Mažuranić 2, HR-35000 Slavonski Brod, Croatia
E-mail: pkonjatic@unisb.hr